Published in final edited form as:
Glia. 2015 April ; 63(4): 635–651. doi:10.1002/glia.22774.

Macrophages in spinal cord injury: phenotypic and functional change from exposure to myelin debris

Xi Wang[1,4,*], **Kai Cao**[1,5,*], **Xin Sun**[1,*], **Yongxiong Chen**[1], **Zhaoxia Duan**[1], **Li Sun**[2], **Lei Guo**[2], **Paul Bai**[1], **Dongming Sun**[1], **Jianqing Fan**[3], **Xijing He**[4], **Wise Young**[1], and **Yi Ren**[2]

[1]W. M. Keck Center for Collaborative Neuroscience, Rutgers, The State University of New Jersey, NJ 08854, USA

[2]Department of Biomedical Sciences, Florida State University, College of Medicine, Tallahassee, FL, 32306, USA

[3]Statistics Laboratory, Princeton University, NJ, 08540, USA

[4]Institute of Neurosciences, the Fourth Military Medical University, Xian 710032, China

[5]Department of Orthopedics Surgery, the 2nd Hospital of Xian Jiaotong University, Xian 710004 China

Abstract

Macrophage activation and persistent inflammation contribute to the pathological process of spinal cord injury (SCI). It was reported that M2 macrophages were induced at 3–7 days after SCI but M2 markers were reduced or eliminated after 1 week. By contrast, M1 macrophage response is rapidly induced and then maintained at injured spinal cord. However, factors that modulate macrophage phenotype and function are poorly understood. We developed a model to distinguished bone marrow derived macrophages (BMDMs) from residential microglia and explored how BMDMs change their phenotype and functions in response to the lesion-related factors in injured spinal cord. Infiltrating BMDMs expressing higher Mac-2 and lower CX3CR1 migrate to the epicenter of injury, while microglia expressing lower Mac-2 but higher CX3CR1 distribute to the edges of lesion. Myelin debris at the lesion site switches BMDMs from M2 phenotype towards M1-like phenotype. Myelin debris activate ATP-binding cassette transporter A1 (ABCA1) for cholesterol efflux in response to myelin debris loading *in vitro*. However, this homeostatic mechanism in injured site is overwhelmed, leading to the development of foamy macrophages and lipid plaque in the lesion site. The persistence of these cells indicates a pro-inflammatory environment, associated with enhanced neurotoxicity and impaired wound healing. These foamy macrophages have poor capacity to phagocytose apoptotic neutrophils resulting in uningested neutrophils releasing their toxic contents and further tissue damage. In conclusion, these data demonstrate for the first time that myelin debris generated in injured spinal cord

Requests for reprints: Dr. Yi Ren, Department of Biomedical Sciences, Florida State University College of Medicine, 1115 West Street, Tallahassee, FL, 32306, USA, Tel: 850 645 2013, Fax: 850 644 5781, yi.ren@med.fsu.edu.
*X. Wang, K. Cao and X. Sun contributed equally to this study.

Conflict of Interest
The authors declare no competing financial interests.

modulates macrophage activation. Lipid accumulation following macrophage phenotype switch contributes to SCI pathology.

Keywords

spinal cord injury; macrophages; myelin debris; foamy cells

Introduction

Spinal cord injury (SCI) provokes an inflammatory response that initially results in further tissue damage and neurodegeneration (Ren and Young 2013). Inflammation can activate resident microglia cells and attract bone marrow derived macrophages (BMDMs), the two major monocytic lineage cell types that contribute to inflammation in SCI (Kim and Joh 2006). However, activated microglia and macrophages in the injured spinal cord can't be distinguished from each other, due to the lack of specific markers. Individual contributions of BMDMs and microglia are not fully understood.

Macrophages are heterogeneous cells with extensive functional plasticity. Macrophages have been classified into two main groups designated M1 and M2 (Gordon 2003; Mantovani et al. 2004). M1 macrophages produce pro-inflammatory cytokines, reactive oxygen species (ROS) and NO, contributing to tissue inflammation and damage. In contrast, M2 macrophages produce anti-inflammatory factors and have a reduced capacity to produce pro-inflammatory molecules, thereby contributing to wound healing and tissue-remodeling. Macrophages have the capacity to switch from one phenotype to another, induced by factors in the inflammatory microenvironment following injury or infection (Mosser and Edwards 2008; Wolfs et al. 2011). In the injured spinal cord, M1 macrophages have a detrimental effect while M2 macrophages promote a regenerative response in adult sensory axons, even in the context of inhibitory substrates that dominate the injury site (David and Kroner 2011; Kigerl et al. 2009). Most macrophages/microglial cells in injured spinal cords are M1 cells and only a transient and small number are M2 (Kigerl et al. 2009). The predominance of M1 macrophages and the low number of M2 macrophages after SCI contribute to the chronic inflammatory response and secondary damage (David and Kroner 2011; Kigerl et al. 2009). Characterization of macrophage phenotypes and the post-SCI chemical microenvironment should clarify how macrophages participate in the pathogenic process of SCI and to pave the way for new therapeutic strategies.

Inflammation contributes to spinal cord damage and demyelination. After SCI, demyelination progresses over long periods (Almad et al. 2011; Totoiu and Keirstead 2005). Accumulating myelin debris containing inhibitory molecules not only inhibit axonal regeneration (Chen et al. 2000; McKerracher et al. 1994), but also act as potent inflammatory stimuli that may contribute to further tissue damage (Jeon et al. 2008; Sun et al. 2010). In the present study, we demonstrated that myelin debris from spinal cord rapidly changed M2 macrophages phenotype. Lipid accumulated in the lesion site, leading to formation of foamy cells and lipid plaques. Macrophages that lost M2 phenotype and took on foamy cell characteristics endured in the lesion site for a long period. These persisting

macrophages were pro-inflammatory, enhanced neurotoxicity, and impaired wound healing. Therefore, our data suggest myelin debris leads to formation of foamy macrophages, which perpetuate the chronic inflammatory response. Interactions between macrophages and myelin debris are likely to play an important role in the inflammatory response in SCI and other demyelinating conditions.

Materials and Methods

Mice strains

All mice were purchased from Jackson Laboratory (Bar Harbor, ME). Mice at age of 8–10 weeks (body weight of 25–28g) were used for the study. Mice were maintained in pathogen-free animal facility at Rutgers University. Animal protocols were approved by Animal Care and Facilities Committee of Rutgers University.

Reagents and antibodies

All chemicals were purchased from Sigma-Aldrich (St. Louis, MO) and cell culture media was purchased from Invitrogen (Carlsbad, CA) unless otherwise indicated. Arginase Assay Kit was purchased from BioAssay Systems (Hayward, CA), and hybridoma cell lines of F4/80 and Mac-2 from American Tissue Culture Collection (ATCC, Manassas, VA). Anti-IBA-1 (ionized calcium binding adapter molecule 1) antibody was purchased from Wako (Osaka, Japan) and anti-Arginase 1 antibody from BD bioscience. Antibodies of anti-Stat3, phospho-Stat3 (Tyr705), GAPDH, NF-κB p65, P-PI3K p85/p55, P-Akt and Stat6 were purchased from Cell Signaling Technology (Danvers, MA). Antibodies of anti-phospho-Stat6 (Tyr641) and PPARγ were from Santa Cruz Biotechnology (Santa Cruz, CA). Anti-YM 1 antibody was purchased from STEMCELL Technologies (Vancouver, BC, Canada). All secondary antibodies were from Invitrogen.

Preparation of myelin debris

Myelin debris was isolated from the brains of 3-month-old mice by sucrose density gradient centrifugation, as described previously (Sun et al. 2010). The endotoxin concentration of myelin debris was below the detection limit by Limulus Amebocyte Lysate assay. Myelin debris was used to stimulate cells with concentration of 100 mg myelin protein per milliliter in all experiments.

Mouse bone marrow-derived macrophages (BMDMs)

Mouse BMDMs from WT mice were prepared as previously described (Wang et al. 2012). Briefly, BM cells from mice 6–8 weeks of age were collected from femoral shafts by flushing the marrow cavity of femurs of with DMEM supplemented with 1% FBS. Cells were cultured for 7 days at a cell density of 1×10^6/ml in 100 mm polystyrene tissue culture dishes containing in DMEM supplemented with 15% conditioned medium from L929 cells (a source of M-CSF) and 10% FBS.

OPC preparation of culture

Mouse OPC from neonatal mouse pups were prepared as described (Xiao et al. 2013). Briefly, cortex from neonatal mouse pups was dissociated and cultured in neurosphere growth medium (NCM) with 20 ng/ml EGF and 20 ng/ml bFGF for 10 days. From the 10th day of the culture, EGF/bFGF were gradually switched to B104 neuroblastoma conditioned medium-containing oligosphere medium to induct oligosphere formation from neurospheres for 14 days. The oligospheres were dissociated and the cells were cultured in the medium containing 10 ng/ml PDGF-AA and 10 ng/ml bFGF for OPC proliferation.

Proliferation assay

Cells were seeded in 96-well plates at a concentration of 1500 cells per well, respectively and cultured for 48h. Plates were fixed with ice-cold 10% trichloroacetic acid (TCA) for 1h and stained with 0.4% sulforhodamine B (SRB, w/v) in 1% v/v acetic acid for 30 min. The mean absorbance at 570 nm was measured using a Universal Microplate Reader (EL800, BIO-TEK Instruments, USA).

Preparation of apoptotic polymorphonuclear neutrophils (PMNs)

Mouse peritoneal PMNs induced by thioglycollate were aged in cultured for 24h in Iscove's DMEM with 10% FBS and PMNs underwent apoptosis spontaneously in culture (Ren et al. 2008). The viability of >99% confirmed by trypan blue exclusion, and apoptosis verified by light microscopy of May-Giemsa-stained cytopreps, showing the typical apoptotic PMN characteristics.

Phagocytosis assay

Apoptotic PMNs were washed twice with PBS, suspended in Iscove's DMEM, and 5×10^5 cells were added to each washed well of macrophages. After interaction for 30 min at 37°C in 5% CO2 atmosphere, the wells were washed in saline at 4°C to remove noningested apoptotic cells. The wells were fixed with 2% glutaraldehyde and then stained for myeloperoxidase to reveal ingested cells. The proportion of macrophages ingesting PMNs was counted using inverted light microscopy.

Histology and immunofluorescence

Mice were transcardially perfused with 0.9% saline followed by 4% paraformaldehyde. Segments of spinal cord encompassing the impact site were removed and fixed in 4% paraformaldehyde for 3h, cryoprotected in 20% sucrose overnight at 4°C, frozen, and cut into 15 microns-thick coronal with a cryostat microtome. The sections were incubated with primary antibodies overnight at 4 °C followed by secondary antibodies at room temperature (RT) for 1 h. Primary antibody omission controls were performed to exclude nonspecific binding. Samples were examined and microphotographs were taken using Zeiss AxioCam microscope and AxioPhot image collection system (Carl Zeiss, Germany) and a confocal Laser Scanning Microscopy (Nikon, Japan). Staining was graded as weak (trace to 1^+) or strong (2 to 3^+).

BM radiation chimeras

C57BL/6 female mice of 8–10 weeks of age were irradiated in a plastic box with 10 Gy X-ray. These mice received an intravenous injection of 5×10^6 bone marrow cells from transgenic mice constitutively expressing GFP/RFP. Efficient reconstitution was confirmed by post-mortern examination of bone marrow and circulating blood for GFP^+ or RFP^+ cells. About 80% the transplants engrafted.

Wound sealing assay

The wound sealing assays on macrophage were performed as described previously (Roney et al. 2011). Brifely, BMDMs were cultured in 24 well plates and scratched with a 200μl micropipette tip. Cells were imaged by Zeiss AxioCam microscope and AxioPhot image collection system at 5 points per scratch. The wound closure was quantified by measuring the remaining unmigrated area using ImageJ. The migration ability was expressed by the percentage of the closure of gap distance using wells of M2 macrophages at 100%.

Spinal cord injury

Female mice of 8–10 weeks of age were used throughout these experiments. We exposed spinal cords by laminectomy at T10, contused the spinal cord with the NYU impactor by dropping a 5-gram rod 6.25 mm onto the spinal cord (Young 2002). Mice contused with asymmetrical injuries were excluded from experimental analysis.

Statistical analysis

Data in figures are presented as mean ± SEM, with n indicating the number of experiments. Statistical significance was evaluated between two individual samples using Student's unpaired t-tests. For multiple comparisons, one-way analysis of variance (ANOVA) followed by Dunnett's post-hoc test. Statistical significance was set at P value < 0.05.

Results

Bone marrow-derived macrophages accumulate at the epicenter of injured spinal cord

In order to determine the distribution of bone marrow-derived macrophages (BMDMs) in the injured spinal cord, we generated chimeric mice in which the bone marrow (BM) cells of the recipient mice were replaced by donor BM cells that express GFP. Thus, most BMDMs in the chimeric mice were green fluorescently labeled. Spinal cord contusion injury was made using a standardized MASCIS NYU impactor in GFP-BM reconstituted mice at 4 weeks after BM replacement. The spinal cords were examined at different time points as indicated after injury (Fig. 1A). Most GFP^+ cells were absent at day 1 after injury but they started to migrate into the injury site at day 3 (Fig. 1A). GFP^+ cells accumulated at the lesion site at 2 weeks after injury and were restricted in lesion center at 8 weeks (Fig. 1A). To further identify these infiltrating BM cells, which accumulated at the lesion site, we double-stained sections for astrocyte marker GFAP (glial fibrillary acidic protein) and the well-characterized membrane macrophage marker F4/80. GFP^+ cells were F4/80 positive (Fig. 1B, C) and these cells accumulated in the GFAP negative lesion site (Fig. 1B, C). In addition, the GFP-positive bone-marrow derived cells (BMDCs) expressed IBA-1 (Figure

1D), another macrophage marker (Ito et al. 2001), and CD68, a lysosomal marker for activated macrophages (Chiu et al. 2009), confirming that these BMDCs were activated macrophages. Almost all the F4/80, CD68, and IBA-1 colocalized with GFP, indicating that a vast majority of macrophages in the lesion site were circulating bone marrow cells rather than locally activated microglia cells.

We used CX3CR1$^{GFP/+}$ knock-in mice to ascertain which macrophages were from locally activated macrophages. CX3CR1 is mainly expressed by monocytes, and resident macrophages/microglial cells. Thus, heterozygous CX3CR1$^{GFP/+}$ mice have CD11b^{+}F4/80^{+} cells which are GFP-positive (Geissmann et al. 2003; Jung et al. 2000). Because CX3CR1 was predominately expressed by resident microglia (Mizutani et al. 2012; Saederup et al. 2010), we reasoned that CX3CR1$^{GFP/+}$ mice would provide direct evidence for the distribution of microglial cells in injured spinal cord. Uninjured control spinal cord contained CX3CR1^{+} microglial cells (Fig. 2A). After SCI, microglial cells expressing strong CX3CR1 (CX3CR1^{+++}) were mainly present in the marginal and uninjured areas and were absent from the lesion site (Fig. 2A). Only CX3CR1 weak positive cells (CX3CR1^{+}) were present in the injury site and these cells also expressed IBA-1 (Fig. 2B). The CX3CR1^{+++}/IBA-1^{+} microglial cells mainly distributed in the edges of the lesion (Fig. 2B). In addition, we transplanted RFP bone marrow cells to lethally irradiated CX3CR1$^{GFP/+}$ mice and contused the spinal cord at 4 weeks later. In these animals, BM cells were RFP^{+} while microglial cells were GFP^{+}. At the lesion site, most RFP^{+} BM cells were F4/80 positive and few GFP^{+} cells were present (Fig. 2C). In contrast, only GFP^{+} microglia were present in the side of the lesion.

BMDMs can be distinguished from microglial cells by Mac-2

We further showed that BMDMs can be distinguished from microglia cells by Mac-2, a beta-galactoside-binding S-type lectin galectin-3 (Yang et al. 2008). Double stained images obtained from CX3CR1$^{GFP/+}$ mouse showed that Mac-2^{+} cells were absent in uninjured cord and at 1 day after injury (Fig. 3A, B). Mac-2^{+} cells appeared at 3 day and peaked 1–2 weeks after injury. These Mac-2^{+} cells were IBA-1 positive but negative or weak positive for CX3CR1 (Fig. 3C). Cell with strong GFP expression (CX3CR1^{+++}) expressed little or no Mac-2 (Mac-2$^{+/-}$) (Fig. 3C, D, E). Mac-2^{+} cells were abundantly present in lesion core and the patterns of distribution were similar to BMDMs (Fig. 3C, D, E). In summary, two distinct populations of CX3CR1^{+}/Mac-2^{+++} and CX3CR1^{+++}/Mac-2$^{+/-}$ cells was visualized in injured spinal cord (Fig. 3D, E), suggesting that residential microglia can be distinguished from recently recruited BMDMs based on the expression of Mac-2.

Appearance of lipid plaque and lipid-laden macrophages in injured spinal cord

“Foamy” macrophages staining positively with oil red O (ORO) are a hallmark of phagocytic activity in atherosclerosis and demyelinative diseases such as experimental allergic encephalomyelitis and multiple sclerosis (Smith 1999). ORO stains only intracellular neutral lipids such as cholesterol ester (CE) but not intact myelin and normal CNS. ORO-positive lesions revealed accumulations of foamy cells in lesion site. Myelin debris exists for long periods of time in the injured spinal cord (Imai et al. 2008; Vargas and Barres 2007) and the debris can be phagocytosed by macrophages. We detected ORO

stained lipid-laden foamy cells in lesion site (Fig. 4). Figure 4A showed representative images of mouse spinal cords at different times after SCI. Lipid-laden cells (foamy cells) were present at 1 week after SCI and concentrated in the lesion core at 4 weeks. The lipid plaques appeared wherever BMDMs were present, suggesting that macrophages took up myelin debris, degraded them to neutral lipids. The lipid plaque was surrounded by the activated microglial cells (Fig. 4B). Confocal images showed many lipid-laden macrophages in the lesion core at 2–4 weeks after injury (Fig. 4C). Electron microscopy confirmed these foamy macrophages contained myelin debris in different stages of degradation, including loose lamellae (red arrow), degrading myelin (green arrow), degraded myelin (purple arrow) and the accumulation of lipid drops (blue arrow) in the cytoplasm (Fig. 4D).

Distribution of M2 and foamy macrophages in early and chronic injured spinal cord

Infiltrating BMDMs have functional plasticity and can change their phenotypes and functions in response to the changing microenvironment (Gordon and Taylor 2005). We examined the activation patterns of macrophages in the injured spinal cord. By using F4/80 and M2 key marker Arginase-1 (Arg-1), we found most F4/80 expressing macrophages colocalized with Arg-1 (Fig. 4E). M2 macrophages peaked at 1 week after SCI (Fig. 4E). However, Arg-1^+ cells were no longer present in the lesion site at 2 weeks (Fig. 4E). The disappearance of Arg-1 correlated with lipid accumulation. Furthermore, expression of CD206, another M2 marker was decreased from 2 week post-injury (Fig. 4F), while expression of M1 marker CD16/32 was markedly enhanced (Fig. 4G). These results are consistent with the study from Kigerl *et al.* reporting that most macrophages/microglial cells are M1 cells, with only a transient and small number showing M2 phenotype (Kigerl et al. 2009).

Myelin debris skews macrophage polarization

The absence of M2 macrophages shortly after SCI suggests that lesion-associated factors (e.g., cytokines, oxygen tension, etc.) cause macrophages to differentiate into M1 macrophages. Kigerl et al (Kigerl et al. 2009) reported that M2 macrophages quickly lost this phenotype when injected into the lesion site, while retaining it in normal spinal cord. It has been shown that apoptosis of oligodendrocytes following SCI is observed at 4–8 days and myelin debris exists for a longer periods of time in the injured spinal cord (Vargas and Barres 2007). We therefore investigated whether myelin debris is one of lesion-associated factors altering the M2 phenotype. We primed BMDMs to an M2 phenotype with M-CSF, the cytokine that drives M2 macrophage activation and promotes anti-inflammatory response (Puig-Kroger et al. 2009; Sierra-Filardi et al. 2010) and then co-cultured M2 macrophages with myelin debris to evaluate its effect on macrophage phenotype and to complement the *in vivo* data. M2 macrophages expressed high levels of well characterized M2 markers including YM1 (a member of chitinase family expressed by M2 macrophages), FIZZ-1 and Arg-1 (Chinetti et al. 2003; Loke et al. 2002; Rauh et al. 2005; Sica et al. 2006) in the presence of M-CSF (Fig. 4H). Treatment of M2 BMDMs with myelin debris led to a significant decrease in the expression of M2 markers. The level of iNOS, an M1 marker, was markedly increased by myelin debris treatment (Fig. 4H). In addition, although myelin did not significantly down regulated expression of CD86, another M1 marker, by using

fluorescence-activated cell sorting (FACS), myelin treatment significantly inhibited M2 marker CD206 (Fig. 4I).

The balance between activation of M1 macrophage–associated NF-κB/STAT1 and M2 macrophage–associated STAT3/STAT6 finely regulates macrophage activity (Sica and Bronte 2007). A predominance of NF-κB/STAT1 activation results in M1 macrophage polarization. In contrast, a predominance of STAT3/STAT6 activation results in M2 macrophage polarization. We therefore examined whether NF-κB/Stat3/6 participated in myelin debris-induced M2 inactivation. Treatment of BMDMs with myelin debris inhibited the activity of Stat3 and stat6 (Fig. 4J) but increased the level of phosphorylated IκB-α (Fig. 4J). These data supported the conclusion that myelin debris induced macrophage M1 activation is associated with inactivation of Stat3 and Stat6 and activation of NF-κB.

ABCA1 expression correlated with myelin lipid efflux *in vitro*

As significant intracellular lipid accumulation in the lesion core, we next studied the expression of ATP-binding cassette transporter A1 (ABCA1), which is responsible to lipid efflux from foamy cells to extracellular lipid acceptors (Lawn et al. 1999). At 1 week after injury, ABCA1 predominantly decorated the plasma membrane and colocalized with Arg-1 and F4/80 (Fig. 5A). However, expression of both Arg-1 and ABCA1 was markedly decreased in the lesion site after 2 weeks (Fig. 5A). We further studied the relationship of intracellular lipid accumulation and macrophage activation *in vitro*. Myelin debris can be taken up by macrophages quickly resulting in the formation of foamy cells (Fig. 5B). Myelin debris-inhibited Arg-1 expression was transient. Decreased Arg-1 activity was only observed 24h after myelin debris uptake (Fig. 5C) when intracellular lipid accumulation was observed (Fig. 5D). However, myelin debris treatments for 24h largely enhanced the levels of ABCA1 and peroxisome proliferator-activator receptor-γ (PPAR-γ), an inducer to regulate ABCA1 expression (Fig. 5E). Myelin-induced lipids can be quickly removed from macrophages within 48–72h (Fig. 5D), suggesting that macrophages have strong capacity to handle accumulated lipids in order to maintain lipid homeostasis. It is reasonable to assume that lipid accumulation resulted in M2 to M1 polarization and M2 activity was restored once lipid content was expelled. Although myelin-derived lipids can be expelled by macrophages *in vitro* within 48–72 hours, foamy macrophages persisted in lesion site for long time after SCI (Fig. 4A). It is possible that injury-derived factors significantly inhibited ABCA1 expression and consequently, myelin-derived lipid exportation was inhibited.

Myelin debris stimulates macrophage expression of pro-inflammatory cytokines

It is reported that myelin-laden macrophages in multiple sclerosis (MS) are anti-inflammatory since they express less proinflammatory cytokines (Boven et al. 2006). If it is the case for SCI, it is not clear why macrophages in the injured spinal cord, which contain large amounts of myelin debris, do not have an anti-inflammatory phenotype (David and Kroner 2011). On the contrary, myelin debris not only accelerated switching from M2 to M1 phenotype, but also significantly enhanced the expression of M1 cytokines (Fig. 6). Incubation of M-CSF-primed M2 macrophages with myelin debris resulted in significantly increased mRNA levels of the pro-inflammatory molecules such as IL-6, MIF, IL-1β, IP-10,

IL-12 and TNF-α (Fig. 6A, B), while control particles such as latex beads and ox-LDL failed to stimulate macrophages express TNF-α (Fig. 6B).

Foamy macrophages are neurotoxic and showed delayed wound healing

It is generally postulated that M2 macrophages promote wound healing and resolution of inflammation (Mantovani et al. 2004). We further investigated whether myelin debris affected macrophage function in would healing. *In vitro* wound healing assay in monolayer cells provides direct measurement for the rate of two-dimensional cell migration. To explore the ability of myelin-laden macrophages to participate in *in vitro* wound healing assay, macrophages were cultured with IFN-γ, IL-4 and myelin debris treatment 24h and macrophage phenotypes were confirmed by expression of Arg-1 (data not shown). Confluent M1, M2 and foamy macrophages were scratched and incubated for the indicated time following wound scratching. As shown in Fig. 7A, M2 macrophages showed a significantly earlier closure of the scratch wound. By contrast, foamy macrophages, like M1 macrophages, were unable to entirely repopulate the wound. Image analysis allowed the quantification of macrophage infiltration to the wound (Fig. 7A). This result demonstrates the function of myelin debris as an inhibitor of macrophage motility, which is essential for wound healing. Furthermore, conditioned medium (CM) from foamy macrophages markedly inhibited survival of oligodendrocyte precursor cells (OPC) (Fig. 7B). This data suggested that foamy macrophages are not anti-inflammatory.

Foamy macrophage lost phagocytic capacity for apoptotic cells

In the injured spinal cord, abundant polymorphonuclear neutrophils (PMNs) infiltrate at 1 day after SCI (Fig. 8A) and accumulation of foamy macrophages that persist for up to 10 weeks after SCI (Fig. 4). *In vitro* assay showed that myelin debris can be quickly taken up by macrophages within 30 minutes to form foamy macrophages (Fig. 5B). We further investigated whether these myelin-induced foamy macrophages lose the ability to take up apoptotic and necrotic PMNs which would release toxic contents to amplify the inflammatory response and induce secondary damage. Apoptotic PMNs were incubated with IFN-γ-induced M1, MCSF-induced M2 and foamy macrophages, respectively. Apoptotic PMNs can be ingested by both M1 and M2 macrophages within 30 minutes (Fig. 8B). However, foamy macrophages lost the ability to take up apoptotic PMNs (Fig. 8B). We further created a simple *in vitro* model of the inflamed site in which normal and foamy macrophages were co-cultured for indicated time with apoptotic PMNs (viability > 98%). Under control condition (Mφ+PMN), after 24h of co-culture only, >80% of total PMNs were quickly taken-up by macrophages (Fig. 8C, D), with PMN viability 95.5% (Fig. 8E) and 62.3% of macrophages ingested PMN (Fig. 8F). There were more PMNs within control macrophages, while fewer PMNs were found in foamy macrophages (Fig. 8C). PMN ingestion by foamy macrophages was markedly impaired, >50% being uningested at every time point we tested (Fig. 8D) and >20% uningested PMNs were necrotic (trypan blue^{+}) (Fig. 8E). By contrast, less than 1% PMNs were necrotic in control group (Mφ+PMN). Only 9.5% of foamy macrophages ingested PMNs (Fig. 8F). Furthermore, myeloperoxidase (MPO), one of major enzymes in PMNs that causes tissue damage was significantly increased in the supernatants from foamy macrophages co-cultured with PMNs (Fig. 8G). MPO levels in the supernatants from control cultures (Mφ+PMN) were almost undetectable

(Fig. 8G). Myelin debris did not affect the enzyme levels in supernatants of either macrophage or PMN culture alone (data not shown). Our results suggest that myelin debris inhibits macrophage uptake of intact apoptotic PMNs, which may result in increased release of cellular contents and cytokines into the inflamed site. These factors may promote a pathogenic pathway leading to persistence rather than resolution of inflammation. In order to understand whether impaired phagocytic capacity is apoptotic cell specific, foamy macrophages were incubated with IgG opsonized zymosan and fluorescent latex beads and fluorescent oxidized low density lipoprotein (ox-LDL) respectively. Ingestion of these particles by foamy macrophages was not affected (Fig. 8H), suggesting that myelin debris only impaired apoptotic cell clearance specifically.

Discussion

Macrophage activation and persistent inflammation are linked to the pathological process of SCI. Macrophages are heterogeneous cells. It has been shown that $CX3CR1^{low}CCR2^{+}Gr1^{+}$ subset, which was termed “inflammatory monocytes” migrate to inflamed tissue from bone marrow. In contrast, $CX3CR1^{high}CCR2^{+}$ $Gr1^{+}$ subset infiltrates to noninflamted tissue (Geissmann et al. 2003). In our present study, we distinguished two macrophage populations and showed they have unique phenotypes and locations. Residential microglia can be distinguished from recently recruited BMDMs based on the expression of Mac-2. BMDMs expressing strong Mac-2 but weak CX3CR1 migrated to injured site while microglial cells distributed to the side of lesion. These two populations of macrophages may have different functions. Residential microglial cells form a border that seems to seal the lesion and block the spread of damage (Hines et al. 2009). In contrast, BMDMs enter the epicenter of injured spinal cord that phagocytose apoptotic and necrotic cells and clear tissue debris such as myelin debris (David and Kroner 2011).

Macrophages have extensive functional plasticity, which allows them to switch from one phenotype to another in the presence of various factors in the inflammatory microenvironment following injury or infection (Mosser and Edwards 2008; Wolfs et al. 2011). M1 macrophages in the injured spinal cord have detrimental effect while M2 macrophages promote a regenerative growth response in adult sensory axons (David and Kroner 2011; Kigerl et al. 2009; Shechter et al. 2009). However, most macrophages/ microglial cells are M1 cells, with only a transient and small number showing M2 (Kigerl et al. 2009). The predominance of M1 macrophages and lower number of M2 macrophages after SCI may contribute to the chronic inflammatory response and secondary damage (David and Kroner 2011; Kigerl et al. 2009). It has been recently shown that TNF-α prevents myelin-laden macrophages from M1 to M2 switch *in vitro* and *in vivo* (Kroner et al. 2014). Although the cytokine milieu is a major determinant of macrophage activation (Gordon and Taylor 2005; Mosser and Edwards 2008), this can be driven by other lesion-related factors as well, seeing as rapid increases in pro-inflammatory cytokines are only detectable in early stage post injury (David and Kroner 2011; Pineau and Lacroix 2007) and pro-inflammatory phenotype persists for a long period of time. We provided novel data exploring the effects of myelin debris by showing that it promotes the macrophage phenotype switch from M2 to M1 like cells demonstrating its pro-inflammatory effects and its potential promotion of secondary damage by function study including delay of wound

healing and impaired capacity for apoptotic and necrotic cell clearance. However, activation microglia/macrophages cannot be regarded as a simple dichotomy of M1 or M2. The reactive phenotype spectrum is actually much broader. Some researchers suggested that macrophages can be classified into six subsets according to their activities: inflammation, phagocytosis, vascular remodeling, matrix rebuilding, regeneration, and immune regulation (Condeelis and Pollard 2006; Hanahan and Weinberg 2000). The most critical observation that requires more focus is the change in function of myelin-laden macrophages, which can ultimately determine their pro- or anti-inflammatory nature.

Contradictory results were reported about induction of inflammatory mediators by myelin phagocytosis. Some studies revealed that myelin phagocytosis induce TNF-α and NO production (Glim et al. 2010; Sun et al. 2010; VanderLaan et al. 1996), while others showed that LPS treated macrophages are insensitive to subsequent myelin stimulation for production of TNF-α and other pro-inflammatory cytokines (Boven et al. 2006; Kroner et al. 2014; Van Rossum et al. 2008). These differences may be due to the differences in the source of myelin (human, bovine, rat, mouse) and macrophages (BMDMs, peritoneal macrophages, human monocytes) (Glim et al. 2010). In our present study, we induced M2 activation by M-CSF (one of M2 activators) first and subsequently stimulated cells with myelin debris. In contrast to the previous study, myelin debris down-regulated M-CSF induced M2 activation. Although inhibition of LPS-induced inflammation can be recognized as anti-inflammatory, our *in vitro* experiments may be more closely mimic *in vivo* SCI. In addition, the microarray data from myelin-laden macrophages did not point towards a typical M2 phenotype (Bogie et al. 2012). Therefore, it is suggested that macrophages stimulated by myelin debris may adopt a novel phenotype that differs from conventional M1 and M2 phenotypes (Bogie et al. 2012; Van Rossum et al. 2008).

Macrophages are consistently expressing ABCA1 which is correlated with lipid efflux (Oram and Heinecke 2005). ABCA1 is not only responsible for cellular cholesterol efflux but also functions to promote the M2 anti-inflammatory phenotype (Yvan-Charvet et al. 2010). Increased intracellular levels of cholesterol ester (CE) activate peroxisome proliferator-activator receptor-γ (PPAR-γ) and the nuclear receptor heterodimer liver X receptor/retinoid X receptor (LXR/RXR), the key regulators of lipid metabolism and inflammation (Bensinger and Tontonoz 2008; Hong and Tontonoz 2008). PPAR-γ/LXR activation induces the expression of ABCA1, as well as other genes involved in lipid efflux such as ABCG1 and ApoE while also increasing expression of anti-inflammatory cytokines and M2 marker, Arg-1 (Bensinger and Tontonoz 2008; Odegaard et al. 2007). Intracellular accumulation of CE activates PPAR-γ/LXR following myelin internalization (Bogie et al. 2012) via scavenger receptors (Rotshenker 2003; Rotshenker et al. 2008; Smith 1999). Activation of PPAR-γ/LXR results in elimination of the intracellular lipids within 48 hours *in vitro* via increased expression of ABCA1. This may be the mechanism by which macrophages maintain lipid homeostasis and which allows them to deal with excessive myelin debris. However, we reported for the first time that there was a striking deficiency of ABCA1 expression and lipid efflux in macrophages occupying the lesion site, which lead to the formation of foamy cells and lipid plaques. This data suggested that ABCA1 was

inhibited by unknown lesion-related factors, which resulted in lipid accumulation and persistent inflammation.

One of characteristics of myelin-induced foamy macrophages is the defective apoptotic/necrotic cell clearance. PMNs are well-known to undergo apoptosis and secondary necrosis spontaneously in a short time (<24h), releasing their cytotoxic contents which harms surrounding tissues. These contents include a variety of digestive enzymes (elastase, collagenase, gelatinase, myeloperoxidase, lysozyme) and cytokines (TNF-α, IL-1β, IL-8, IP-10 and MIP-1α) (Kasama et al. 2005). Removal of apoptotic PMNs is the prerequisite of the resolution of inflammation (Ren and Savill 1998). Normally, infiltrating PMNs can be cleared by tissue macrophages or BMDMs and thus release of their noxious contents is prevented. Defective apoptotic PMN clearance may be responsible for chronic inflammatory response (Ren and Savill 1998; Ren et al. 2003; Savill et al. 2002) and therefore may contribute to secondary injury after SCI. We showed that large numbers of PMNs entered the injury site within 24h. Although PMN number decreased after 1 day, PMNs persisted in the core for up to 6 months after SCI and remain for weeks and even months (Beck et al. 2010; Kigerl et al. 2006; Nguyen et al. 2011), suggesting continuing PMN infiltration or impaired PMN clearance because PMNs are absent in the uninjured spinal cord and do not replicate in tissue. Both M1 and M2 macrophages can ingest apoptotic cells while foamy macrophages cannot (Fig. 8). Uningested PMNs leads to the release of toxic contents and subsequent amplification of the inflammatory response and resultant secondary damage. These observations suggest a new mechanism of secondary injury that has previously not been proposed and will stimulate the development of new treatment strategies for treatment of SCI. However, future study is needed to understand the mechanisms by which myelin debris impairs the ability of macrophage to phagocytose apoptotic cells.

Our data suggested that foamy macrophages may contribute to the development of secondary injury. Thus, promotion of intracellular lipid efflux would be expected to inhibit secondary injury. Moreover, high extracellular cholesterol levels are essential for myelin membrane growth (Saher et al. 2005), and this cholesterol is made locally, not imported into the CNS (Jurevics and Morell 1995). Therefore boosting cholesterol efflux not only reduces foamy cell formation and inflammation but also provides cholesterol for remyelination. Recent studies showed that both rosiglitazone and pioglitazone, PPAR-γ specific agonists, are extremely neuroprotective in animal models of acute CNS insults including SCI and surgical trauma (Hyong et al. 2008; McTigue et al. 2007; Park et al. 2007; Pereira et al. 2006; Zhao et al. 2006). Furthermore, statins, widely used for cholesterol-lowering therapy and prevention of atherosclerosis-related events (Istvan and Deisenhofer 2001), not only enhance ABCA1 expression but also have an anti-inflammatory effect by blocking Rho GTPases. Atorvastatin (brand name: Lipitor), a widely used statin, inhibited lipid accumulation in macrophages incubated with VLDL. When used *in vitro*, Atorvastatin enhances phagocytic activity of macrophages and is blood-brain barrier (BBB)-permeable. Atorvastatin for acute SCI has been reported to inhibit the inflammatory response and have neuroprotective effects and was shown to facilitate significant behavioral recovery in three studies from two laboratories (Kwon et al. 2011). Our results explain why statins and PPAR-

γ agonists have shown so much promise in treating SCI. Therefore, combination of boosting phagocytosis capacity and lipid efflux may be a more effective intervention for SCI.

Acknowledgments

This work was supported by the National Science Foundation (DMS-0714589 to Y.R.); National Institutes of Health (R01GM100474-01 to J.F. and Y.R.), a Joyce and Les Goodman scholarship (to Y. R.), the New Jersey Commission on Spinal Cord Research (CSCR13IRG006 to Y. R. and W.Y.) and the National Natural Science Foundation of China (81171156 to X.W).

Abbreviation

Arg-1	Arginase-1
ABCA1	ATP-binding cassette transporter A1
BMDCs	bone-marrow derived cells
BMDMs	bone marrow derived macrophages
CM	conditioned medium
GFAP	glial fibrillary acidic protein
M-CSF	macrophage colony stimulating factor
MPO	myeloperoxidase
OPC	oligodendrocyte precursor cell
ORO	oil red O
PMN	neutrophils
PPAR-γ	peroxisome proliferator-activator receptor-γ
SCI	spinal cord injury

References

Almad A, Sahinkaya FR, McTigue DM. Oligodendrocyte fate after spinal cord injury. Neurotherapeutics. 2011; 8(2):262–73. [PubMed: 21404073]

Beck KD, Nguyen HX, Galvan MD, Salazar DL, Woodruff TM, Anderson AJ. Quantitative analysis of cellular inflammation after traumatic spinal cord injury: evidence for a multiphasic inflammatory response in the acute to chronic environment. Brain. 2010; 133(Pt 2):433–47. [PubMed: 20085927]

Bensinger SJ, Tontonoz P. Integration of metabolism and inflammation by lipid-activated nuclear receptors. Nature. 2008; 454(7203):470–7. [PubMed: 18650918]

Bogie JFJ, Timmermans S, Van Anh H-T, Irrthum A, Smeets HJM, Gustafsson J-A, Steffensen KR, Mulder M, Stinissen P, Hellings N, et al. Myelin-Derived Lipids Modulate Macrophage Activity by Liver X Receptor Activation. Plos One. 2012; 7(9)

Boven LA, Van Meurs M, Van Zwam M, Wierenga-Wolf A, Hintzen RQ, Boot RG, Aerts JM, Amor S, Nieuwenhuis EE, Laman JD. Myelin-laden macrophages are anti-inflammatory, consistent with foam cells in multiple sclerosis. Brain. 2006; 129(Pt 2):517–26. [PubMed: 16364958]

Chen MS, Huber AB, van der Haar ME, Frank M, Schnell L, Spillmann AA, Christ F, Schwab ME. Nogo-A is a myelin-associated neurite outgrowth inhibitor and an antigen for monoclonal antibody IN-1. Nature. 2000; 403(6768):434–9. [PubMed: 10667796]

Chinetti G, Fruchart JC, Staels B. Peroxisome proliferator-activated receptors: new targets for the pharmacological modulation of macrophage gene expression and function. Curr Opin Lipidol. 2003; 14(5):459–68. [PubMed: 14501584]

Chiu IM, Phatnani H, Kuligowski M, Tapia JC, Carrasco MA, Zhang M, Maniatis T, Carroll MC. Activation of innate and humoral immunity in the peripheral nervous system of ALS transgenic mice. Proc Natl Acad Sci U S A. 2009; 106(49):20960–5. [PubMed: 19933335]

Condeelis J, Pollard JW. Macrophages: Obligate partners for tumor cell migration, invasion, and metastasis. Cell. 2006; 124(2):263–266. [PubMed: 16439202]

David S, Kroner A. Repertoire of microglial and macrophage responses after spinal cord injury. Nat Rev Neurosci. 2011; 12(7):388–99. [PubMed: 21673720]

Geissmann F, Jung S, Littman DR. Blood monocytes consist of two principal subsets with distinct migratory properties. Immunity. 2003; 19(1):71–82. [PubMed: 12871640]

Glim JE, Vereyken EJF, Heijnen DAM, Vallejo JJG, Dijkstra CD. The Release of Cytokines by Macrophages Is Not Affected by Myelin Ingestion. Glia. 2010; 58(16):1928–1936. [PubMed: 20830806]

Gordon S. Alternative activation of macrophages. Nat Rev Immunol. 2003; 3(1):23–35. [PubMed: 12511873]

Gordon S, Taylor PR. Monocyte and macrophage heterogeneity. Nat Rev Immunol. 2005; 5(12):953–64. [PubMed: 16322748]

Hanahan D, Weinberg RA. The hallmarks of cancer. Cell. 2000; 100(1):57–70. [PubMed: 10647931]

Hines DJ, Hines RM, Mulligan SJ, Macvicar BA. Microglia processes block the spread of damage in the brain and require functional chloride channels. Glia. 2009; 57(15):1610–8. [PubMed: 19382211]

Hong C, Tontonoz P. Coordination of inflammation and metabolism by PPAR and LXR nuclear receptors. Curr Opin Genet Dev. 2008; 18(5):461–7. [PubMed: 18782619]

Hyong A, Jadhav V, Lee S, Tong W, Rowe J, Zhang JH, Tang J. Rosiglitazone, a PPAR gamma agonist, attenuates inflammation after surgical brain injury in rodents. Brain Res. 2008; 1215:218–24. [PubMed: 18479673]

Imai M, Watanabe M, Suyama K, Osada T, Sakai D, Kawada H, Matsumae M, Mochida J. Delayed accumulation of activated macrophages and inhibition of remyelination after spinal cord injury in an adult rodent model. J Neurosurg Spine. 2008; 8(1):58–66. [PubMed: 18173348]

Istvan ES, Deisenhofer J. Structural mechanism for statin inhibition of HMG-CoA reductase. Science. 2001; 292(5519):1160–4. [PubMed: 11349148]

Ito D, Tanaka K, Suzuki S, Dembo T, Fukuuchi Y. Enhanced expression of Iba1, ionized calcium-binding adapter molecule 1, after transient focal cerebral ischemia in rat brain. Stroke. 2001; 32(5):1208–15. [PubMed: 11340235]

Jeon SB, Yoon HJ, Park SH, Kim IH, Park EJ. Sulfatide, a major lipid component of myelin sheath, activates inflammatory responses as an endogenous stimulator in brain-resident immune cells. J Immunol. 2008; 181(11):8077–87. [PubMed: 19018000]

Jung S, Aliberti J, Graemmel P, Sunshine MJ, Kreutzberg GW, Sher A, Littman DR. Analysis of fractalkine receptor CX(3)CR1 function by targeted deletion and green fluorescent protein reporter gene insertion. Mol Cell Biol. 2000; 20(11):4106–14. [PubMed: 10805752]

Jurevics H, Morell P. Cholesterol for synthesis of myelin is made locally, not imported into brain. J Neurochem. 1995; 64(2):895–901. [PubMed: 7830084]

Kasama T, Miwa Y, Isozaki T, Odai T, Adachi M, Kunkel SL. Neutrophil-derived cytokines: potential therapeutic targets in inflammation. Curr Drug Targets Inflamm Allergy. 2005; 4(3):273–9. [PubMed: 16101533]

Kigerl KA, Gensel JC, Ankeny DP, Alexander JK, Donnelly DJ, Popovich PG. Identification of two distinct macrophage subsets with divergent effects causing either neurotoxicity or regeneration in the injured mouse spinal cord. J Neurosci. 2009; 29(43):13435–44. [PubMed: 19864556]

Kigerl KA, McGaughy VM, Popovich PG. Comparative analysis of lesion development and intraspinal inflammation in four strains of mice following spinal contusion injury. J Comp Neurol. 2006; 494(4):578–94. [PubMed: 16374800]

Kim YS, Joh TH. Microglia, major player in the brain inflammation: their roles in the pathogenesis of Parkinson's disease. Exp Mol Med. 2006; 38(4):333–47. [PubMed: 16953112]

Kroner A, Greenhalgh AD, Zarruk JG, Passos Dos Santos R, Gaestel M, David S. TNF and Increased Intracellular Iron Alter Macrophage Polarization to a Detrimental M1 Phenotype in the Injured Spinal Cord. Neuron. 2014; 83(5):1098–116. [PubMed: 25132469]

Kwon BK, Okon E, Hillyer J, Mann C, Baptiste D, Weaver LC, Fehlings MG, Tetzlaff W. A systematic review of non-invasive pharmacologic neuroprotective treatments for acute spinal cord injury. J Neurotrauma. 2011; 28(8):1545–88. [PubMed: 20146558]

Lawn RM, Wade DP, Garvin MR, Wang X, Schwartz K, Porter JG, Seilhamer JJ, Vaughan AM, Oram JF. The Tangier disease gene product ABC1 controls the cellular apolipoprotein-mediated lipid removal pathway. J Clin Invest. 1999; 104(8):R25–31. [PubMed: 10525055]

Loke P, Nair MG, Parkinson J, Guiliano D, Blaxter M, Allen JE. IL-4 dependent alternatively-activated macrophages have a distinctive in vivo gene expression phenotype. BMC Immunol. 2002; 3:7. [PubMed: 12098359]

Mantovani A, Sica A, Sozzani S, Allavena P, Vecchi A, Locati M. The chemokine system in diverse forms of macrophage activation and polarization. Trends Immunol. 2004; 25(12):677–86. [PubMed: 15530839]

McKerracher L, David S, Jackson DL, Kottis V, Dunn RJ, Braun PE. Identification of myelin-associated glycoprotein as a major myelin-derived inhibitor of neurite growth. Neuron. 1994; 13(4):805–11. [PubMed: 7524558]

McTigue DM, Tripathi R, Wei P, Lash AT. The PPAR gamma agonist Pioglitazone improves anatomical and locomotor recovery after rodent spinal cord injury. Exp Neurol. 2007; 205(2):396–406. [PubMed: 17433295]

Mizutani M, Pino PA, Saederup N, Charo IF, Ransohoff RM, Cardona AE. The fractalkine receptor but not CCR2 is present on microglia from embryonic development throughout adulthood. J Immunol. 2012; 188(1):29–36. [PubMed: 22079990]

Mosser DM, Edwards JP. Exploring the full spectrum of macrophage activation. Nat Rev Immunol. 2008; 8(12):958–69. [PubMed: 19029990]

Nguyen HX, Beck KD, Anderson AJ. Quantitative assessment of immune cells in the injured spinal cord tissue by flow cytometry: a novel use for a cell purification method. J Vis Exp. 2011; (50)

Odegaard JI, Ricardo-Gonzalez RR, Goforth MH, Morel CR, Subramanian V, Mukundan L, Red Eagle A, Vats D, Brombacher F, Ferrante AW, et al. Macrophage-specific PPARgamma controls alternative activation and improves insulin resistance. Nature. 2007; 447(7148):1116–20. [PubMed: 17515919]

Oram JF, Heinecke JW. ATP-binding cassette transporter A1: a cell cholesterol exporter that protects against cardiovascular disease. Physiol Rev. 2005; 85(4):1343–72. [PubMed: 16183915]

Park SW, Yi JH, Miranpuri G, Satriotomo I, Bowen K, Resnick DK, Vemuganti R. Thiazolidinedione class of peroxisome proliferator-activated receptor gamma agonists prevents neuronal damage, motor dysfunction, myelin loss, neuropathic pain, and inflammation after spinal cord injury in adult rats. J Pharmacol Exp Ther. 2007; 320(3):1002–12. [PubMed: 17167171]

Pereira MP, Hurtado O, Cardenas A, Bosca L, Castillo J, Davalos A, Vivancos J, Serena J, Lorenzo P, Lizasoain I, et al. Rosiglitazone and 15-deoxy-Delta12,14-prostaglandin J2 cause potent neuroprotection after experimental stroke through noncompletely overlapping mechanisms. J Cereb Blood Flow Metab. 2006; 26(2):218–29. [PubMed: 16034372]

Pineau I, Lacroix S. Proinflammatory cytokine synthesis in the injured mouse spinal cord: multiphasic expression pattern and identification of the cell types involved. J Comp Neurol. 2007; 500(2):267–85. [PubMed: 17111361]

Puig-Kroger A, Sierra-Filardi E, Dominguez-Soto A, Samaniego R, Corcuera MT, Gomez-Aguado F, Ratnam M, Sanchez-Mateos P, Corbi AL. Folate receptor beta is expressed by tumor-associated macrophages and constitutes a marker for M2 anti-inflammatory/regulatory macrophages. Cancer Res. 2009; 69(24):9395–403. [PubMed: 19951991]

Rauh MJ, Ho V, Pereira C, Sham A, Sly LM, Lam V, Huxham L, Minchinton AI, Mui A, Krystal G. SHIP represses the generation of alternatively activated macrophages. Immunity. 2005; 23(4):361–74. [PubMed: 16226502]

Ren Y, Savill J. Apoptosis: the importance of being eaten. Cell Death Differ. 1998; 5(7):563–8. [PubMed: 10200510]

Ren Y, Tang J, Mok MY, Chan AW, Wu A, Lau CS. Increased apoptotic neutrophils and macrophages and impaired macrophage phagocytic clearance of apoptotic neutrophils in systemic lupus erythematosus. Arthritis Rheum. 2003; 48(10):2888–97. [PubMed: 14558095]

Ren Y, Xie Y, Jiang G, Fan J, Yeung J, Li W, Tam PK, Savill J. Apoptotic cells protect mice against lipopolysaccharide-induced shock. J Immunol. 2008; 180(7):4978–85. [PubMed: 18354223]

Ren Y, Young W. Managing inflammation after spinal cord injury through manipulation of macrophage function. Neural Plast. 2013; 2013:945034. [PubMed: 24288627]

Roney KE, O'Connor BP, Wen H, Holl EK, Guthrie EH, Davis BK, Jones SW, Jha S, Sharek L, Garcia-Mata R, et al. Plexin-B2 negatively regulates macrophage motility, Rac, and Cdc42 activation. PLoS One. 2011; 6(9):e24795. [PubMed: 21966369]

Rotshenker S. Microglia and macrophage activation and the regulation of complement-receptor-3 (CR3/MAC-1)-mediated myelin phagocytosis in injury and disease. J Mol Neurosci. 2003; 21(1): 65–72. [PubMed: 14500997]

Rotshenker S, Reichert F, Gitik M, Haklai R, Elad-Sfadia G, Kloog Y. Galectin-3/MAC-2, Ras and PI3K activate complement receptor-3 and scavenger receptor-AI/II mediated myelin phagocytosis in microglia. Glia. 2008; 56(15):1607–13. [PubMed: 18615637]

Saederup N, Cardona AE, Croft K, Mizutani M, Cotleur AC, Tsou CL, Ransohoff RM, Charo IF. Selective chemokine receptor usage by central nervous system myeloid cells in CCR2-red fluorescent protein knock-in mice. PLoS One. 2010; 5(10):e13693. [PubMed: 21060874]

Saher G, Brugger B, Lappe-Siefke C, Mobius W, Tozawa R, Wehr MC, Wieland F, Ishibashi S, Nave KA. High cholesterol level is essential for myelin membrane growth. Nat Neurosci. 2005; 8(4): 468–75. [PubMed: 15793579]

Savill J, Dransfield I, Gregory C, Haslett C. A blast from the past: clearance of apoptotic cells regulates immune responses. Nat Rev Immunol. 2002; 2(12):965–75. [PubMed: 12461569]

Shechter R, London A, Varol C, Raposo C, Cusimano M, Yovel G, Rolls A, Mack M, Pluchino S, Martino G, et al. Infiltrating blood-derived macrophages are vital cells playing an anti-inflammatory role in recovery from spinal cord injury in mice. PLoS Med. 2009; 6(7):e1000113. [PubMed: 19636355]

Sica A, Bronte V. Altered macrophage differentiation and immune dysfunction in tumor development. J Clin Invest. 2007; 117(5):1155–66. [PubMed: 17476345]

Sica A, Schioppa T, Mantovani A, Allavena P. Tumour-associated macrophages are a distinct M2 polarised population promoting tumour progression: potential targets of anti-cancer therapy. Eur J Cancer. 2006; 42(6):717–27. [PubMed: 16520032]

Sierra-Filardi E, Vega MA, Sanchez-Mateos P, Corbi AL, Puig-Kroger A. Heme Oxygenase-1 expression in M-CSF-polarized M2 macrophages contributes to LPS-induced IL-10 release. Immunobiology. 2010; 215(9–10):788–95. [PubMed: 20580464]

Smith ME. Phagocytosis of myelin in demyelinative disease: a review. Neurochem Res. 1999; 24(2): 261–8. [PubMed: 9972873]

Sun X, Wang X, Chen T, Li T, Cao K, Lu A, Chen Y, Sun D, Luo J, Fan J, et al. Myelin activates FAK/Akt/NF-kappaB pathways and provokes CR3-dependent inflammatory response in murine system. PLoS One. 2010; 5(2):e9380. [PubMed: 20186338]

Totoiu MO, Keirstead HS. Spinal cord injury is accompanied by chronic progressive demyelination. J Comp Neurol. 2005; 486(4):373–83. [PubMed: 15846782]

Van Rossum D, Hilbert S, Strassenburg S, Hanisch U-K, Brueck W. Myelin-phagocytosing macrophages in isolated sciatic and optic nerves reveal a unique reactive phenotype. Glia. 2008; 56(3):271–283. [PubMed: 18069669]

VanderLaan LJW, Ruuls SR, Weber KS, Lodder IJ, Dopp EA, Dijkstra CD. Macrophage phagocytosis of myelin in vitro determined by flow cytometry: Phagocytosis is mediated by CR3 and induces production of tumor necrosis factor-alpha and nitric oxide. Journal of Neuroimmunology. 1996; 70(2):145–152. [PubMed: 8898723]

Vargas ME, Barres BA. Why is Wallerian degeneration in the CNS so slow? Annu Rev Neurosci. 2007; 30:153–79. [PubMed: 17506644]

Wang X, Chen T, Leng L, Fan J, Cao K, Duan Z, Zhang X, Shao C, Wu M, Tadmori I, et al. MIF produced by bone marrow-derived macrophages contributes to teratoma progression after embryonic stem cell transplantation. Cancer Res. 2012; 72(11):2867–78. [PubMed: 22461508]

Wolfs IM, Donners MM, de Winther MP. Differentiation factors and cytokines in the atherosclerotic plaque micro-environment as a trigger for macrophage polarisation. Thromb Haemost. 2011; 106(5):763–71. [PubMed: 21947328]

Xiao L, Hu C, Yang W, Guo D, Li C, Shen W, Liu X, Aijun H, Dan W, He C. NMDA receptor couples Rac1-GEF Tiam1 to direct oligodendrocyte precursor cell migration. Glia. 2013; 61(12): 2078–99. [PubMed: 24123220]

Yang RY, Rabinovich GA, Liu FT. Galectins: structure, function and therapeutic potential. Expert Rev Mol Med. 2008; 10:e17. [PubMed: 18549522]

Young W. Spinal cord contusion models. Prog Brain Res. 2002; 137:231–55. [PubMed: 12440371]

Yvan-Charvet L, Wang N, Tall AR. Role of HDL, ABCA1, and ABCG1 transporters in cholesterol efflux and immune responses. Arterioscler Thromb Vasc Biol. 2010; 30(2):139–43. [PubMed: 19797709]

Zhao Y, Patzer A, Herdegen T, Gohlke P, Culman J. Activation of cerebral peroxisome proliferator-activated receptors gamma promotes neuroprotection by attenuation of neuronal cyclooxygenase-2 overexpression after focal cerebral ischemia in rats. FASEB J. 2006; 20(8):1162–75. [PubMed: 16770015]

Main points

Myelin debris generated in injured spinal cord switches macrophages from M2 phenotype towards M1-like phenotype and results in the formation of foamy cells and lipid plaques. Foamy macrophages are pro-inflammatory because they are neurotoxic, defective apoptotic/necrotic cell clearance and showed delayed wound healing.

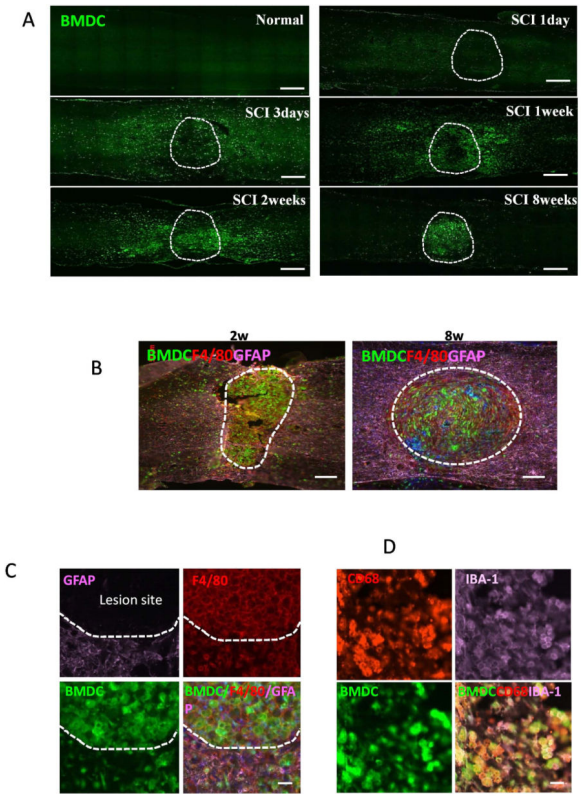

Figure 1. Distribution of bone marrow-derived cells (BMDCs) in the injured spinal cord in WT mice reconstituted with GFP$^+$ BM cells

All BMDCs were GFP$^+$. Dashed lines mark the lesion site. **A.** Distribution of BMDCs in spinal cord sections at indicated time after SCI. **B–C.** Immunostaining analysis showing BMDCs were positive to macrophage marker F4/80 staining (red) in lesion site delineated by GFAP (purple) expression at 2 and 8 weeks (B) and 2 weeks after injury (C). **D.** BMDCs were double positive for IBA-1 (purple) and CD68 (red) staining in lesion site at 2 weeks after injury. Bars: (A) 400 μm; (B) 200 μm; (C, D) 20 μm.

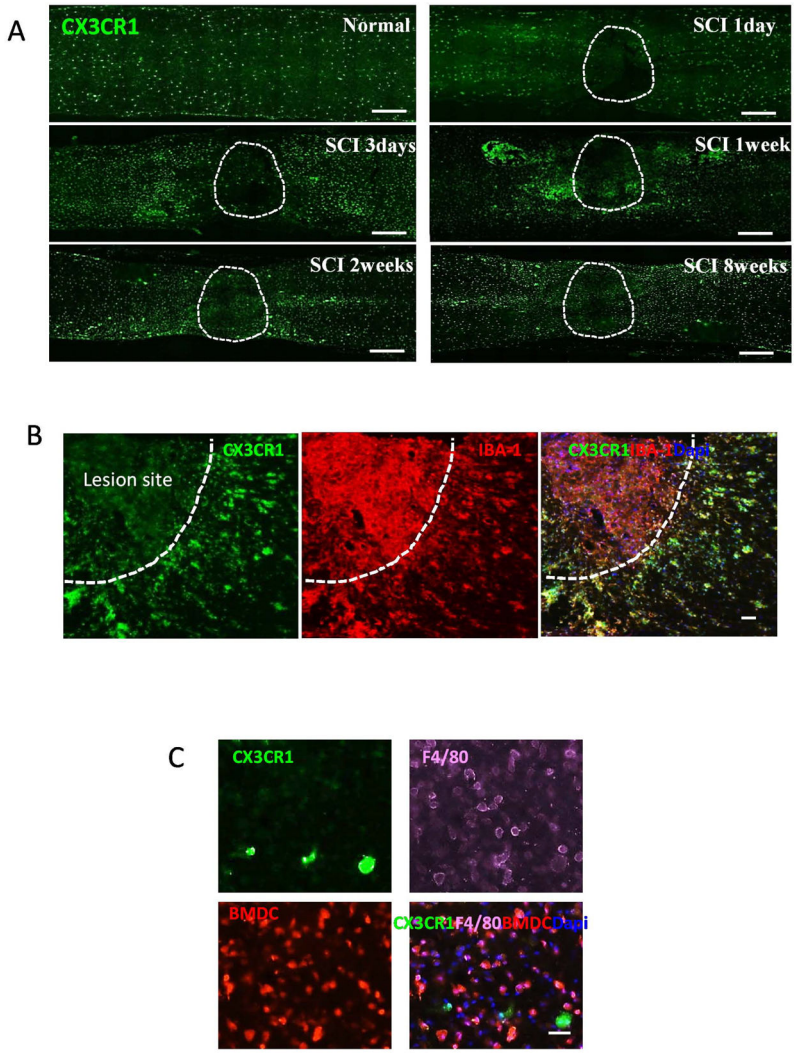

Figure 2. Distribution of microglial cells and BMDCs in the injured spinal cord in CX3CR1$^{GFP/+}$ mice (A and B) or CX3CR1$^{GFP/+}$ mice reconstituted with RFP^{+} BM cells (C)

All microglial cells were CX3CR1^{high}. Dashed lines mark the lesion site. **A.** Distribution of microglial cells (CX3CR1^{high}) in spinal cord sections from CX3CR1$^{GFP/+}$ mice at indicated time after SCI. **B.** Distribution of CX3CR1^{high} and CX3CR1^{low} cells in spinal cord from CX3CR1$^{GFP/+}$ mice at 2 weeks after injury. Both populations were positive for IBA-1 staining (red). **C.** Distribution of microglial cells and BMDCs in the lesion site in CX3CR1$^{GFP/+}$ mice reconstituted with RFP^{+} BM cells at 2 weeks after injury. Sections were labeled with F4/80 antibody (purple). Bars: (A) 400 μm; (B) 40 μm; (C) 30 μm.

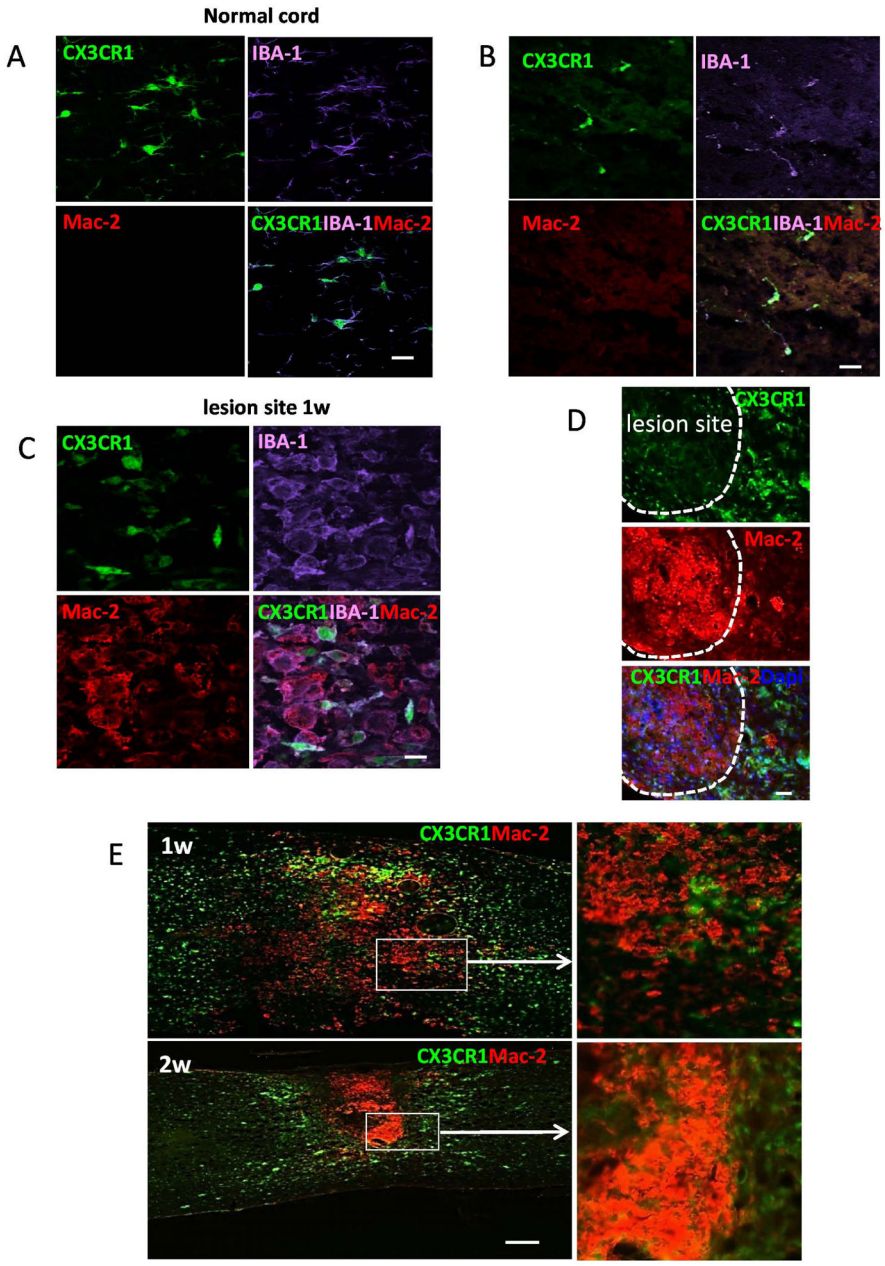

Figure 3. Expression of Mac-2 (red) in the injured spinal cord in CX3CR1$^{GFP/+}$ mice

All microglial cells were CX3CR1^{high}. Dashed lines mark the lesion site. **A–B.** Microglial cells expressed IBA-1 (purple) but Mac-2 was not detected in normal cord (A) and in lesion site at 1 day after injury (B). **C.** Mac-2 was mainly co-localized with IBA-1 (purple) in the lesion site at 1 week after injury. CX3CR1^{high} microglial cells were Mac-2 negative or weak positive. **D.** Mac-2^{+} macrophages mainly restricted in the lesion site at 2 weeks after injury. **E.** Distribution of Mac-2^{+} macrophages in the spinal cord at 1 (upper) and 2 weeks (lower) after injury. The right panel was enlarged images. Bars: (A–C) 20 μm; (D) 40 μm; (E) 400 μm.

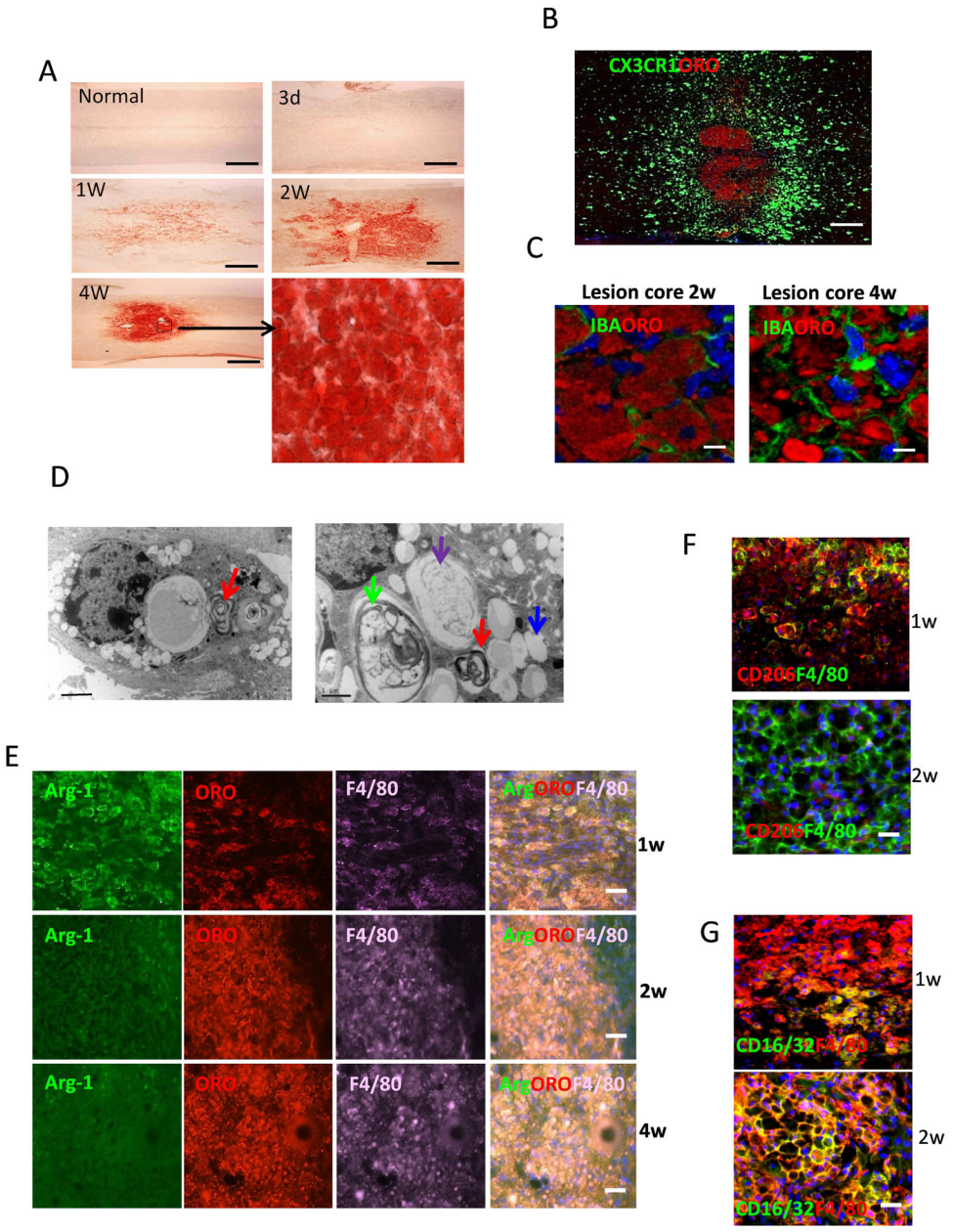

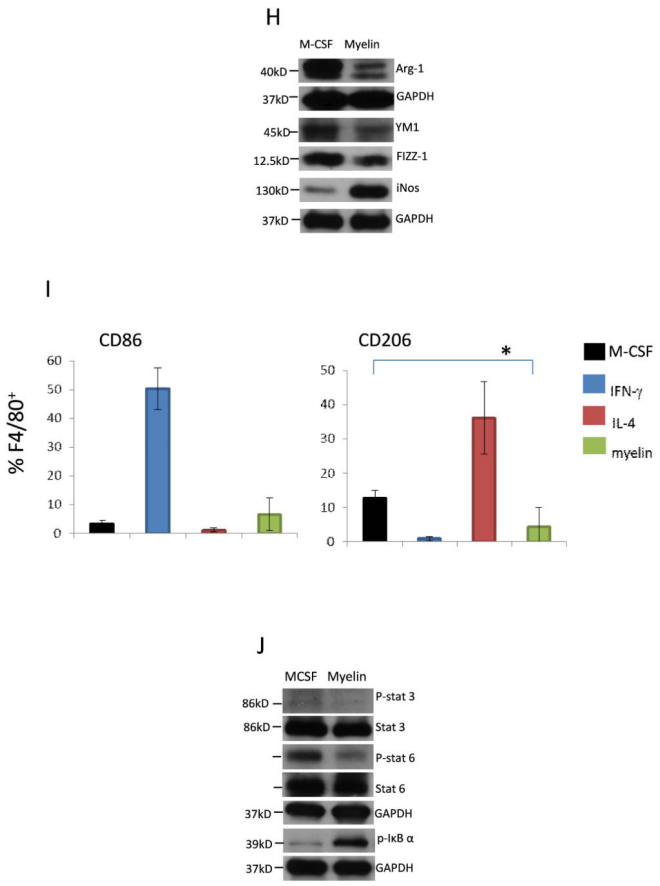

Figure 4. Lipid plaque and foamy cells in lesion site

A. Microscopic images for Oil-red O (ORO) staining of spinal cord at indicated time after SCI. The lower right picture was enlarged image. **B.** ORO staining of spinal cord from CX3CR1$^{GFP/+}$ mice at 6w after SCI. **C.** Confocal images of spinal cord in lesion site at 2 and 4 weeks after SCI. Sections were stained with ORO and IBA-1 (green). **D.** Electron micrographs of macrophages in the lesion site in WT mice at 2 week after injury. **E.** Representative images of immunostaining of sections at indicated time after injury showing double-staining for arginase-1 (Arg-1, green), F4/80 (purple) and ORO (red) in lesion site. **F**. Representative images of immunostaining of sections at indicated time after injury showing double-staining for CD206 (red) and F4/80 (green) in lesion site. **G**. Representative images of immunostaining of sections at indicated time after injury showing double-staining for CD16/32 (green) and F4/80 (red) in lesion site. **H.** M-CSF pre-treated BMDMs were incubated with myelin debris for 24h and M2/M1 markers were assessed by Western blot. **I.** M-CSF pre-treated BMDMs were incubated with IFN-γ, IL-4 and myelin debris for 24h and CD86 and CD206 were detected by flow cytometry (n=3, *P<0.05, two-sided Wilcoxon test). Data are represented as means ± SEM of three independent experiments done in duplicate. **J.** Phosphorylation of Stat3 (p-Stat3), p-Stat6 and p-IκB-α in M-CSF pre-treated BMDMs that incubated with myelin debris. Bars: (A) 400 μm; (B) 300 μm; (C) 5μm; (D) left image 2 μm and right image 1 μm and (E–G) 40 μm.

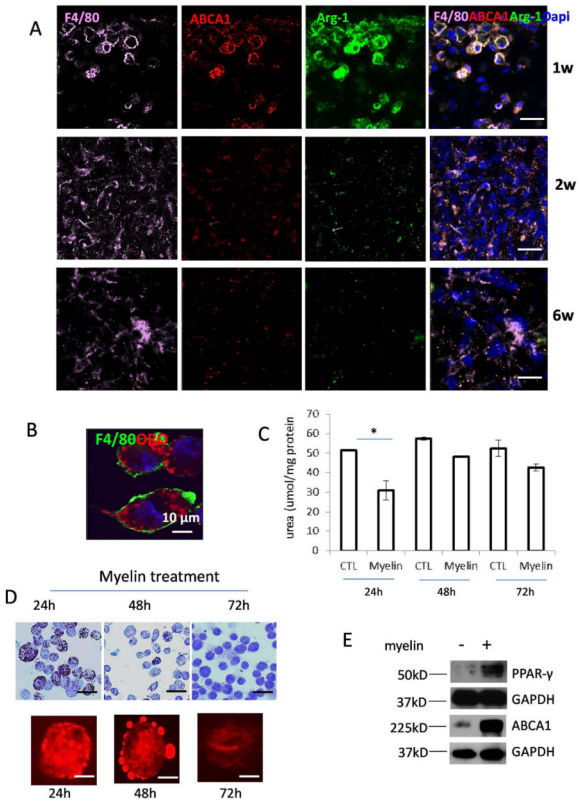

Figure 5. ABCA1 expression *in vivo* and *in vitro*

A. Immunohistochemical analysis of expression of ABCA1 (red) and Arg-1 (green) in macrophages ($F4/80^+$ cells, purple) in lesion site at indicated time points after SCI. **B.** BMDMs ingestion of myelin debris *in vitro*. BMDMs were incubated with myelin debris for 1h and non-ingested myelin debris was washed away. Cells were continued to culture for 24h and stained with ORO (red) and F4/80 (green). **C.** Colorimetric assay to test Arg-1 activity in BMDMs treated with medium alone (CTL) and myelin debris for indicated time (n=3, *P<0.05, two-sided Wilcoxon test). Data are represented as means ± SEM of three independent experiments done in duplicate. **D.** BMDMs were incubated with myelin debris for indicated time and stained with ORO (red). The lower panel is enlarged images for single cell. **E.** BMDMs were incubated in the presence or absence of myelin debris for 24h and PPAR-γ and ABCA1 were assessed by Western blot. Bars: (A) 20 μm. (B) 10 μm; (D) upper image 40 μm and lower image 10 μm.

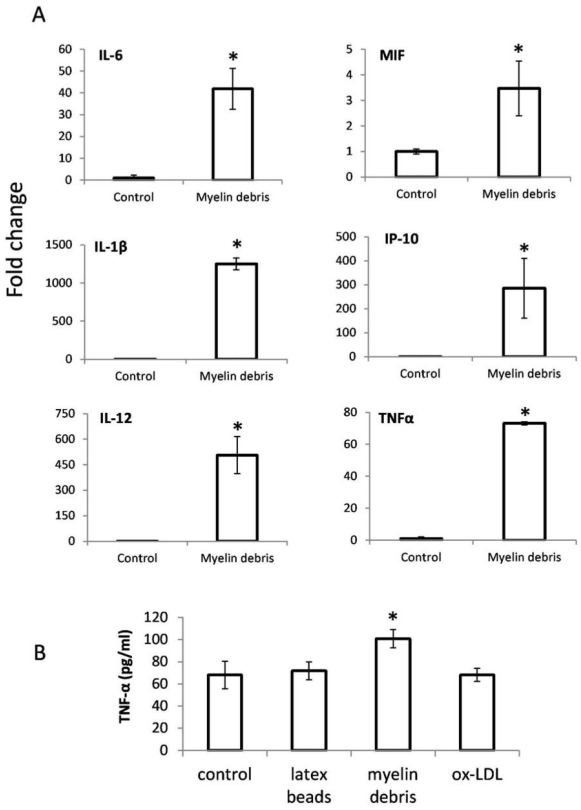

Figure 6. Cytokine expression in response to myelin debris

BMDMs treated with myelin debris for 12h and mRNA expression of IL-6, MIF, IL-1β, IP-10, IL-12 and TNF-α was detected by qRT-PCR. **B.** BMDMs treated with latex beads, myelin debris and ox-LDL for 24h and expression of TNF-α was detected by ELISA. n=3, *P<0.05, two-sided Wilcoxon test. Data are represented as mean ± SEM.

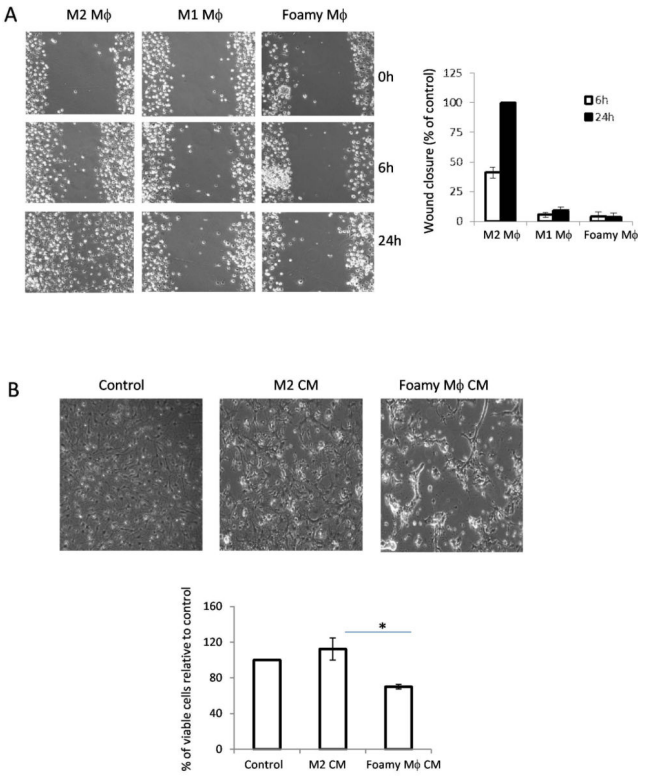

Figure 7. Effect of foamy macrophages on oligodendrocyte precursor cells (OPC) and wound closure

A. Scratch wound-healing assay was conducted in M2 macrophages (Mφ treated with M-CSF, 10ng/ml), M1 Mφ (IFN-γ 10ng/ml) and foamy Mφ (treated with myelin debris). Migration distance was measured at 0, 6, 24 h after cells were scratched (magnification 10×). The migration ability was expressed by the percentage of the closure of gap distance using wells of M2 macrophages at 100%. The results of counted migrated cells were representative of three experiments each done in triplicate. **B.** The growth and morphology of oligodendrocyte precursor cells (OPC) treated with conditioned medium (CM) from control, M2 and foamy macrophages for 48h, respectively (magnification 10×). The quantification of counted viable cells was assessed by SRB assay. n=3, *$p<0.05$, two-sided Wilcoxon test. Data are represented as mean ± SEM.

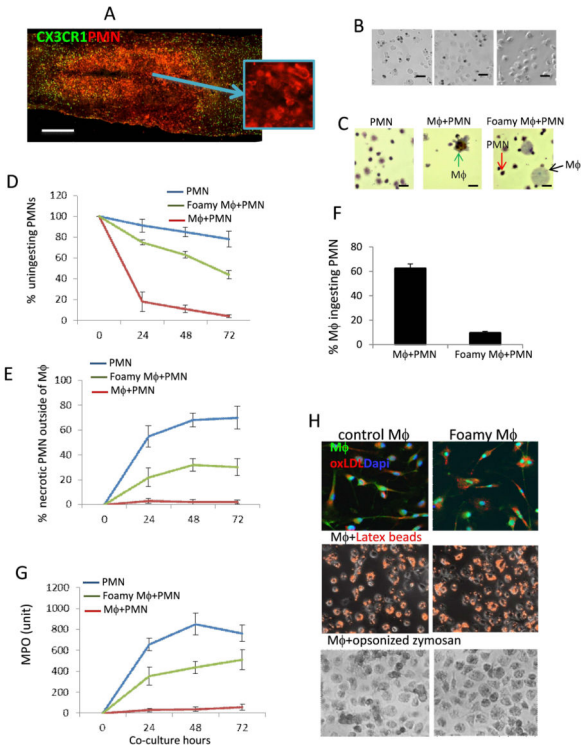

Figure 8. Phagocytic capacity of foamy macrophages for apoptotic PMNs

A. Immunohistochemical analysis showing PMNs (red) in the injury site at 24h after SCI in CX3CR1$^{GFP/+}$ mice. **B.** Phagocytosis capacity of M1, M2 and foamy macrophages for PMNs (magnification 20×). M-CSF induced M1, IL-4 induced M2 and myelin debris induced foamy macrophages were incubated with apoptotic PMNs for 30 min, respectively. Non-ingested apoptotic PMNs were washed away and PMNs within Mφ were positive with MPO staining (black). **C.** *In vitro* model to study the interaction of macrophages, PMNs and myelin debris. Macrophages were incubated with PMNs for 24h in the presence or absence of myelin debris. PMNs were stained with MPO (dark brown). In 24h co-culture, more uningested PMNs (red arrow) and fewer PMNs within foamy Mφ (black arrow) in foamy Mφ+PMN co-culture compared to Mφ+PMN co-culture. More ingested PMNs within Mφ (green arrow) were observed in Mφ+PMN co-culture. **D.** The quantification of counted uningested PMNs in three groups. **E**. Increased the number of trypan blue positive necrotic PMNs in foamy Mφ+PMN co-culture group compared to Mφ+PMN group. **F.** Phagocytosis of apoptotic PMNs by normal and foamy Mφ. **G.** MPO level in the supernatants from co-culture system at indicated time points. **H.** No defective phagocytosis of ox-LDL, latex beads and opsonized zymoson by foamy Mφ. Mφ incubated with ox-LDL-RFP (upper), latex beads-RFP (middle) and opsonized zymoson (lower) for 30 min. Non-ingested particles were washed away. All results were representative of three experiments each done in triplicate. Data are represented as mean ± SEM. (A) 500 μm. (B) 40 μm; (C) 10 μm.